Solar Energy Materials and Solar Cells 200 (2019) 109968

Contents lists available at ScienceDirect

Solar Energy Materials and Solar Cells

journal homepage: www.elsevier.com/locate/solmat

Excessive light-induced degradation in boron-doped Cz silicon PERC triggered by dark annealing

F. Fertig*, R. Lantzsch, F. Frühauf, F. Kersten, M. Schütze, C. Taubitz, J. Lindroos, J.W. Müller

Hanwha Q CELLS GmbH, Sonnenallee 17-21, D-06766, Bitterfeld-Wolfen, Germany

ARTICLE INFO

Keywords:
Boron-oxygen
PERC
Destabilisation
LID

ABSTRACT

This work investigates the impact of annealing at elevated temperatures on the light-induced degradation (LID) of passivated emitter and rear cells (PERC) processed on boron-doped Czochralski-grown silicon substrates. The boron-oxygen (BO) defect has been stabilised prior to annealing and subsequent LID treatment. Excessive LID of up to 19.1 $\%_{rel.}$ is observed upon illumination after extended dark annealing at 150 °C for 552 h, which is well above the BO defect-related LID of 5.6 $\%_{rel.}$ measured upon illumination after cell processing if BO is not stabilised. Light and elevated Temperature Induced Degradation (LeTID), iron-boron pairs and surface recombination are excluded as root causes for the observed increased LID, which shows a similar behaviour as the BO defect but which cannot be explained by the well-established three-state model of the BO defect with the assumption of an empty regenerated state prior to BO stabilisation. Two speculative hypothesis for an explanation are (i) that further BO defect precursors are formed, which could be described via a reservoir or (ii) that a high percentage of the in-principle available BO defects are already in the stabilised state even without dedicated BO defect stabilisation. This increased LID does not occur when at least a small level of excess carrier concentration is induced during extended annealing and, hence, is expected not to occur during field operation. However, the observed behaviour is highly relevant for accelerated aging testing such as, e.g., damp heat testing during IEC and UL certification.

1. Introduction

One prominent root cause for light-induced degradation (LID) in state-of-the-art passivated emitter and rear cells (PERC [1]) on boron-doped Czochralski-grown silicon substrates (*p*-type Cz-Si) is the boron-oxygen (BO) defect [2–5]. The different states of the BO defect are typically described by a three-state-model [6], with the states being referred to as “annealed” (A), “degraded” (B) and “regenerated” (C) or similar, synonymous denominations. For transition conditions in-between states and corresponding rates, please refer to, e.g., Refs. [7–9]. State C is considered “stable” during carrier injection at room temperature while it can be “destabilised” at elevated temperatures without carrier injection [6,10]. Besides the empirically determined correlation of BO defect concentration to boron and oxygen concentrations [11], solar cell processing and the thermal history of the substrate have been discussed to change BO defect concentration [12–19]. Please refer to, e.g., Ref. [9] for discussions of the potential microscopic origin of the BO defect. However, it is often assumed that the total BO defect concentration remains constant after cell processing and is “simply” being re-distributed among states A, B and C depending on the treatment conditions. On lifetime samples, it has been shown that dark annealing can impact the total BO defect density [13]. By transferring the entire BO defect concentration from the recombination-inactive state A to the recombination-active state B, the BO defect usually leads to a degradation of PERC conversion efficiency (A→B) in the order of 4 $\%_{rel.}$ to 6 $\%_{rel.}$ [20], when using state-of-the art *p*-type Cz-Si substrates with typical base doping concentrations in the order of $N_A = 5{\cdot}10^{15}\mathrm{cm}^{-3}$ to $2{\cdot}10^{16}\mathrm{cm}^{-3}$.

This work investigates the impact of annealing at elevated temperatures on the LID of *p*-type Cz-Si PERC that have been subjected to BO stabilisation treatment.

2. Approach

Cz-Si PERC have been manufactured (texture → diffusion → edge isolation → dielectric surface passivation → local contact opening → screen-printed metallisation) in an industrial pilot line on *p*-type Cz-Si substrates with $N_A \approx 2{\cdot}10^{16}\mathrm{cm}^{-3}$ including BO stabilisation. Note that the investigated solar cells do not contain features of Hanwha Q CELLS' Q.ANTUM technology [20–23], i.e. PERC ≠ Q.ANTUM. To check the

* Corresponding author.
E-mail address: f.fertig@q-cells.com (F. Fertig).

https://doi.org/10.1016/j.solmat.2019.109968
Received 29 March 2019; Received in revised form 22 May 2019; Accepted 24 May 2019
Available online 24 June 2019
0927-0248/

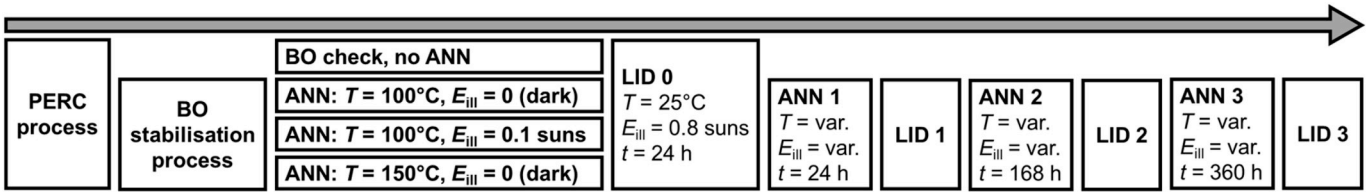

Fig. 1. Sketch of the experimental setup. The impact of iron-boron pairs is excluded by dark storage at room temperature for > 12 h before every measurement.

impact of BO defect concentration upon cell processing, the BO defect has not been stabilised in some cells. The energy conversion efficiency of the fabricated cells before annealing and LID treatment has been ~22.0 %. Fig. 1 shows a sketch of the experimental setup. Annealing at elevated temperatures (ANN) of T = 100 °C and 150 °C has been performed in two ways: (i) in the dark to emulate accelerated aging testing in the laboratory and (ii) under low-intensity illumination with an illumination intensity of E_{ill} = 0.1 suns to emulate injection conditions at maximum power point and, therefore, field conditions (modules typically only exhibit temperatures of T > 30 °C during the day). The investigated cells that have been annealed in the dark at 100 °C have been *IV*- and suns-V_{oc}-tested [24] at different times after annealing and all investigated cells upon subsequent "LID treatment" with E_{ill} = 0.8 suns at a temperature of 25 °C for 24 h. While these conditions trigger BO defect formation (A→B) [9], Light and elevated Temperature Induced Degradation (LeTID) [20,23,25,26] is deactivated [27]. The impact of association and dissociation of iron-boron pairs is excluded by dark storage at room temperature for > 12 h before every measurement.

3. Results

The average initial degradation in maximum output power P_{MPP} of the non-stabilised and stabilised PERC after one LID treatment is 5.6 % and 0.4 %, respectively. Hence, the BO defect concentration after cell processing can lead to a degradation in the expected range given in the previous section and the applied BO defect stabilisation has resulted in most BO defects being in the configuration of state C. Fig. 2 shows results of the conducted experiment. As relative degradation $\Delta P_{MPP}{}^{*}$, the product of short-circuit current density j_{sc}, open-circuit voltage V_{oc} and pseudo fill factor *pFF* is displayed to be consistent since some measurements suffered from fluctuations in contacting and, hence, measured series resistance. When this has not been the case, the relative degradation in fill factor *FF* and *pFF* has been almost identical (deviation of < 0.2 % in $\Delta P_{MPP}{}^{*}$). It can be seen that with increasing annealing time the LID of the investigated cells steadily increases upon illumination due to destabilisation of the BO defect (C→A,B). However, for a cumulated annealing time of 522 h at 100 °C, a relative degradation of 9.2 % is measured upon LID, which is significantly higher than the value of 5.6 % due to the initial BO defect activation determined from non-stabilised cells. When illuminating during the performed annealing at 100 °C, a final LID value of 0.8 % is measured and therefore no significant increase of LID is observed when providing at least a small level of excess carrier injection. When subjecting the cells to an even higher temperature of 150 °C during dark annealing, the destabilisation of the BO defect progresses significantly faster, resulting in a measured LID value of 19.1 %.

4. Discussion

The observed LID is reversed by dark annealing at 100 °C and activated at 25 °C under illumination. While LeTID has been reported to be activated and a reservoir of inactive defects being tapped at extended dark annealing at elevated temperatures [28,29], the observed increased LID within this experiment occurs after illumination at 25 °C – by these conditions, it has been shown that LeTID is not activated but, on the contrary, deactivated [27]. Hence, it is concluded that LeTID is highly unlikely to be the root cause for the observed behaviour. Since no increased LID is observed when providing at least a small level of excess carrier injection, and since dark annealing almost resets $P_{MPP}{}^{*}$ to its initial value, an impact of the surface passivation on the observed LID is considered unlikely, and the observed phenomenon is attributed to a bulk defect. Hence, the observed excessive LID exhibits the same characteristics that would be expected for the BO defect. A similar behaviour has also been observed for Cz substrates from other substrate suppliers and on substrates with different base doping concentrations.

When assuming that the additional LID is due to BO defect formation, two potential explanations can be speculated about: (i) Further BO defect precursors are formed by extended dark annealing, which could be described via a BO defect reservoir that is tapped during dark annealing. (ii) A significant part of the in-principle available BO defect concentration has already been in the configuration of the regenerated state C after cell processing even without applying dedicated BO defect stabilisation treatment. That is, the measured LID value of 5.6 $\%_{rel.}$ w/o BO stabilisation treatment represents "only" a comparably small fraction of the in-principle available BO defect concentration. By extended dark annealing, the BO defect concentration in the degraded state B can therefore be further increased and results in significantly higher LID.

When comparing the results of this study with previous work, Wilking et al. have observed a higher defect concentration than expected for the destabilisation of fired and regenerated lifetime samples with dark annealing in the temperature range of T = 170 °C to 245 °C, which, however, was attributed to a degradation of surface passivation [10]. Furthermore, in the very first submission on the regeneration of the BO defect by Herguth et al. [6], a V_{oc} loss of 30 mV is shown upon destabilisation at T = 170 °C and 180 °C of regenerated "standard industrial-type solar cells", which appears to be higher than the initial BO-induced V_{oc} degradation of ~12 mV to 20 mV displayed in the remainder of the study. Concerning the destabilisation of PERC, Fertig et al. have not observed LID higher than the non-regenerated level for damp-heat testing at 85°C for 1500 h (DH1500) [30] while the data of Hieslmair indicate a destabilisation-induced LD of ≈5.4 $\%_{rel.}$ triggered by dark annealing at 160 °C for ≈45 h starting at an initial efficiency of ≈20.5 % [31]. While Hieslmair comments that "destabilisation appears not to be complete" the displayed data seem to at least approach saturation. In summary, one could speculate that partially a larger than expected BO defect concentration triggered by extended dark annealing may have been previously observed on fired lifetime samples and cells although the origin of the increased BO defect concentration might have been surface passivation degradation [10] or different sample characteristics [6]. In other studies, no increase in LID beyond the expected BO-defect level has been observed since the destabilisation time and/or temperature might have been too low [30] or since the BO-defect induced LID of non-regenerated cells is unclear as a reference [31].

Both Walter et al. [13] and Nampalli et al. [14] have postulated an additional reservoir state "D" based on dark annealing and rapid thermal annealing treatments of lifetime samples, which has been incorporated into a generalised BO defect model by Herguth and Hallam [32]. Nampalli et al. have reported a decrease in BO defect concentration upon a firing step independent of total thermal budget, which in principle points in a similar direction as early studies on the impact of thermal treatment on BO defect concentration, e.g. Refs.

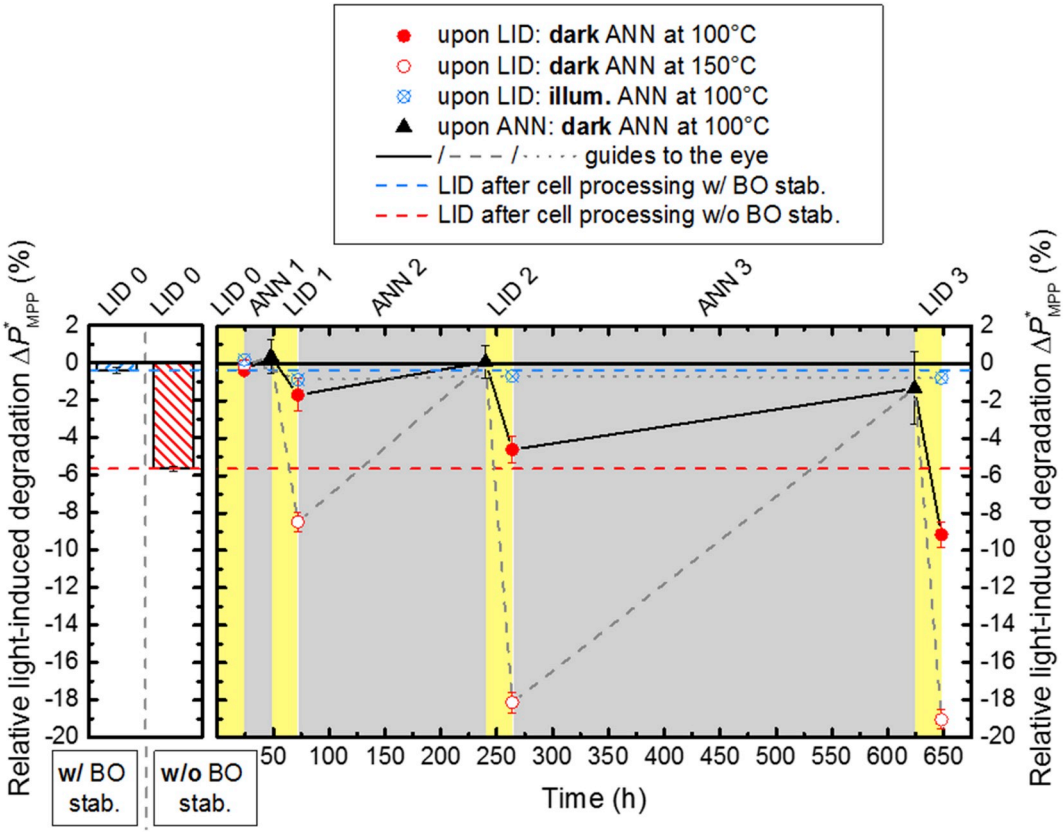

Fig. 2. Relative LID of maximum output power $P_{MPP}^{*} = j_{sc} \cdot V_{oc} \cdot pFF$ for the treatment sketched in Fig. 1. Note that measurements after annealing have been performed for group "dark ANN at 100 °C" only. Error bars represent standard deviations.

[15–19]. These studies will be discussed in more detail below. Walter et al., on the contrary, have observed an increase in BO defect concentration with decreasing dark annealing temperature in the range of 200 °C to 425 °C while sample preparation has not involved a firing step. While both studies support a fourth reservoir state in analogy to hypothesis (i), an increase in BO defect concentration due to dark annealing after a cell-like process including a concluding firing step has not been conclusively reported to date to the knowledge of the authors. While the investigated temperature range in this study is lower than the one investigated by Walter et al., similar maximum degradation results in the range of 19 % to 20 % have been obtained for T_{ANN} = 200 °C and T_{ANN} = 150 °C (results for 200 °C not explicitly shown in section 3), which would rather be expected for hypothesis (ii). However, more temperature-dependent data need to be generated in this temperature range. While Nampalli et al. state that the last temperature ramp is essential for the thermal deactivation of BO defects rather than thermal budget, the results of this study clearly indicate the additional BO defect generation to be due to thermal budget and not temperature ramps.

As stated in the previous paragraph, in previous studies the BO defect concentration has been reported to be reduced in lifetime samples, which have been subjected to high-temperature processing such as diffusion, oxidation, or rapid thermal annealing compared with samples prepared from as-cut wafers that have not been subjected to high-temperature processing [12–19]. Many early studies have reported an increase in BO-defect-related excess carrier lifetime by high-temperature processing, typically in the order of a factor of 2 to 4, e.g. Refs. [15–19]. To not underestimate the BO defect limit of charge carrier lifetime during device modeling, this process-induced decrease in BO defect concentration is typically accounted for by an enhancement factor in the parameterisation of BO-defect-related Shockley-Read-Hall lifetime, refer to, e.g., Eq. (9) in Ref. [33]. With hypothesis (ii) stated previously, these findings could be very speculatively interpreted that BO defects are partially transferred to the configuration of the regenerated state during high-temperature processing, which results in a lower available BO defect density when switching between the annealed and degraded state (A→B) by standard light soaking and annealing. By applying an extended dark anneal at elevated temperatures as performed in this study, the available BO defects could therefore be reset to the state prior to high-temperature processing, significantly increasing the active BO defect concentration, or in principle even beyond the state of the as-cut wafer if already after crystallisation a certain fraction of the BO defect was present in the configuration of the regenerated state C. With hypothesis (ii), also the findings of early studies that the BO defect concentration can be switched between the annealed and degraded state (A→B→A→ …) by alternating dark annealing and light soaking without increasing the BO defect concentration could be explained, since the investigated samples have not been subjected to high-temperature processing [34]. The last paragraphs are highly speculative but should emphasize that the observed results can in principle be explained by hypothesis (i) or (ii), or a combination. Further research is necessary for clarification.

While the applied extended annealing leads to significantly increased LID when performed in the dark, LID is not increased as long as at least a small level of excess carrier injection is provided during annealing, refer to Fig. 2 "illum. ANN at 100 °C". Since modules typically only exhibit temperatures of $T >$ 30 °C during the day, LID is not expected to increase during field operation. However, during IEC and UL module certification testing [35,36] extended dark annealing is applied with the goal to test the durability of module components. If an increased degradation after such a treatment is observed, this degradation may not necessarily point towards module component degradation but could be an artefact of the BO defect destabilisation discussed in this study and the observed degradation would depend on the light exposure before *IV* testing. Hence, certification testing could fail although

the applied conditions are not relevant in the field in terms of LID. A prominent example for such tests is damp-heat testing at 85 °C in the dark, which has been shown to lead to destabilisation of the regenerated state C in previous studies [30,31]. Kersten et al. have confirmed the destabilisation during DH testing and show that it does not occur under simultaneous current injection [37] in analogy to the results reported in this study. In Ref. [37], remedies for BO defect artefacts during certification testing are suggested.

5. Conclusion

This study reports excessive light-induced degradation (LID) of passivated emitter and rear cells (PERC) processed on boron-doped Czochralski-grown silicon substrates triggered by dark annealing at elevated temperatures. Note that the investigated solar cells do not contain features of Hanwha Q CELLS' Q.ANTUM technology, i.e. PERC ≠ Q.ANTUM. Despite stabilisation of the boron-oxygen (BO) defect prior to annealing and LID, LID values of up to 19.1 $\%_{rel.}$ upon illumination after extended dark annealing at 150 °C for 552 h are observed, which is well above the BO defect-related LID of 5.6 $\%_{rel.}$ measured upon illumination after cell processing if the BO defect is not stabilised. Light and elevated Temperature Induced Degradation (LeTID), iron-boron pairs and surface recombination are excluded as root causes for the observed increased LID, which shows a similar behaviour as the BO defect but which cannot be explained by the well-established three-state model of the BO defect with the assumption of an empty regenerated state prior to BO defect stabilisation. Two hypothesis to explain the observed effect are discussed: (i) Further BO defect precursors are formed via a BO defect reservoir and (ii) a significant part of the in-principle available BO defect concentration has already been in the configuration of the regenerated state after cell processing even without applying dedicated BO defect stabilisation treatment. To clarify whether the observed results are due to hypothesis (i) or (ii), or a combination, further research is necessary. Furthermore, it is found that LID is not increased when at least a small level of excess carrier concentration is induced during extended annealing and, hence, is expected not to occur during field operation. However, the observed behaviour is highly relevant for accelerated aging testing such as, e.g., damp heat testing during IEC and UL certification.

Acknowledgements

The authors acknowledge the staff of the Reiner Lemoine Research Center, Cell and Module Pilot Line and Module Test Center at Hanwha Q CELLS for their contribution to this work.

References

[1] A.W. Blakers, et al., Appl. Phys. Lett. 55 (13) (1989) 1363.
[2] S. Rein, et al., Proc. of the 17th EUPVSEC, Munich, Germany, 2001, pp. 1555–1560.
[3] J. Schmidt, K. Bothe, Phys. Rev. B 69 (2) (2004) 24107.
[4] V.V. Voronkov, R. Falster, J. Appl. Phys. 107 (5) (2010) 53509.
[5] H. Fischer, W. Pschunder, Proc. of the 10th IEEE PVSC, Palo Alto, CA, USA, 1973, pp. 404–411.
[6] A. Herguth, et al., Proc. of the 4th WCPEC, Waikoloa, HI, USA, 2006, pp. 940–943.
[7] A. Herguth, G. Hahn, J. Appl. Phys. 108 (11) (2010) 114509.
[8] A. Herguth, S. Wilking, Energy Procedia 124 (2017) 60–65.
[9] T. Niewelt, et al., IEEE J. Photovoltaics (2016) 1–16.
[10] S. Wilking, et al., Sol. Energy Mater. Sol. Cell. 131 (2014) 2–8.
[11] K. Bothe, R. Sinton, J. Schmidt, Prog. Photovoltaics Res. Appl. 13 (4) (2005) 287–296.
[12] D.C. Walter, et al., Appl. Phys. Lett. 104 (4) (2014) 42111.
[13] D.C. Walter, et al., Sol. Energy Mater. Sol. Cell. 173 (2017) 33–36.
[14] N. Nampalli, et al., Sol. Energy Mater. Sol. Cell. 173 (2017) 12–17.
[15] S.W. Glunz, et al., Proc. of the 2nd WCPEC, Vienna, Austria, 1998, pp. 1343–1346.
[16] K. Bothe, et al., Proc. of the 29th IEEE PVSC, New Orleans, LA, USA, 2002, pp. 194–197.
[17] S.W. Glunz, et al., J. Appl. Phys. 90 (5) (2001) 2397–2404.
[18] J. Youn Lee, et al., Prog. Photovoltaics Res. Appl. 9 (6) (2001) 417–424.
[19] J. Knobloch, et al., Proc. of the 13th EUPVSEC, Nice, France, 1995, pp. 9–12.
[20] F. Fertig, et al., Energy Procedia 124 (2017) 338–345.
[21] P. Engelhart, et al., Proc. of the 26th EUPVSEC, Hamburg, Germany, 2011, pp. 821–826.
[22] A. Mohr, et al., Proc. of the 26th EUPVSEC, Hamburg, Germany, 2011, pp. 2150–2153.
[23] F. Kersten, et al., Sol. Energy Mater. Sol. Cell. 142 (2015) 83–86.
[24] R.A. Sinton, A. Cuevas, Proc. of the 16th EUPVSEC, Glasgow, UK, 2000, pp. 1152–1155.
[25] K. Ramspeck, et al., Proc. of the 27th EUPVSEC, Frankfurt, Germany, 2012, pp. 861–865.
[26] F. Fertig, K. Krauß, S. Rein, phys. stat. sol. (RRL) 9 (1) (2015) 41–46.
[27] F. Kersten, et al., Proc. of the 31st EUPVSEC, Hamburg, Germany, 2015, pp. 1822–1826.
[28] D. Chen, et al., Sol. Energy Mater. Sol. Cell. 172 (2017) 293–300.
[29] T.H. Fung, et al., Sol. Energy Mater. Sol. Cell. 184 (2018) 48–56.
[30] F. Fertig, et al., Sol. Energy Mater. Sol. Cell. 121 (2014) 157–162.
[31] H. Hieslmair, Proc. of 26th Workshop on Crystalline Silicon Solar Cells & Modules: Materials and Processes, Vail, CO, USA, 2016.
[32] A. Herguth, B. Hallam, AIP Conference Proceedings 1999, 2018 130006.
[33] P.P. Altermatt, J. Comput. Electron. 10 (3) (2011) 314–330.
[34] J. Schmidt, et al., Proc. of the 26th IEEE PVSC, Anaheim, CA, USA, 1997, pp. 13–18.
[35] International Std IEC 61215, Crystalline Si Terrestrial PV Modules - Design Qualification and Type Approval, (2005).
[36] Standard for Flat-Plate Photovoltaic Modules and Panels, UL1703, (2002).
[37] F. Kersten, et al., Presented at 9th Silicon PV, Leuven, Belgium, 2019.